The Second Revision for ***SBB12467***

Divergent assemblage patterns and driving forces for bacterial and fungal communities along a glacier forefield chronosequence

Yonglei JIANG [1, 3, ‡], Yanbao LEI [1, ‡], Yan YANG [1],

Helena KORPELAINEN [4], Ülo NIINEMETS [5], Chunyang LI [2, *]

[1] *Key Laboratory of Mountain Surface Processes and Ecological Regulation, Institute of Mountain Hazards and Environment, Chinese Academy of Sciences, Chengdu 610041, China*

[2] *College of Life and Environmental Sciences, Hangzhou Normal University, Hangzhou 310036, China*

[3] *University of Chinese Academy of Sciences, Beijing 100039, China*

[4] *Department of Agricultural Sciences, Viikki Plant Science Centre, P.O. Box 27, FI-00014 University of Helsinki, Finland*

[5] *Institute of Agricultural and Environmental Sciences, Estonian University of Life Sciences, Kreutzwaldi 1, 51014 Tartu, Estonia*

‡ These authors contributed equally to this work

* *Correspondence:*

Chunyang LI, E-mail: licy@hznu.edu.cn; Tel: 86-571-28860603; Fax: 86-571-28862256

Original Research Article

Received 17 July 2017

27 text pages, 4 figures with 3 supplementary tables and 4 supplementary figures

Abstract Despite the ubiquitous distributions and critical ecological functions of microorganisms in pedogenesis and ecosystem development in recently deglaciated areas, there are contrasting successional trajectories among bacteria and fungi, but the driving forces of community assembly still remain poorly resolved. In this study, we analyzed both bacterial and fungal lineages associated with seven different stages in the *Hailuogou Glacier Chronosequence*, to quantify their taxonomic composition and successional dynamics, and to decipher the relative contribution from the bottom-up control of soil nutrients and altered vegetation as well as top-down pressures from nematode grazers. Co-occurrence networks showed that the community complexity for both bacteria and fungi typically peaked at the middle chronosequence stages. The overlapping nodes mainly belonged to Proteobacteria and Acidobacteria in bacteria, and Ascomycota and Basidiomycota in fungi, which was further supported by the indicator species analysis. Variation in partitioning and structural equation modeling suggested that edaphic properties were the primary agents shaping microbial community structures, especially at the early stages. The importance of biotic factors, including plant richness and nematode feeding, increased during the last two stages along with the establishment of a coniferous forest, eventually governing the turnover of fungal communities. Moreover, bacterial communities exhibited a more compact network topology during assembly, thus supporting determinism, whereas the looser clustering of fungal communities illustrated that they were determined more by stochastic processes. These pieces of evidence collectively reveal divergent successional trajectories and driving forces for soil bacterial and fungal communities along a glacier forefield chronosequence.

Key words: bacterial community assembly; driving forces; edaphic and biotic properties; fungal community assembly; *Hailuogou Glacier Chronosequence*; stochastic and deterministic processes.

1. Introduction

Microbes are usually the first colonizers and keystone players to elicit a cascade of processes crucial for the development of higher-trophic level food webs, especially in many pristine environments, including glacier retreat areas (Bradley et al., 2016). Despite their ubiquity in terrestrial ecosystems and importance in ecological functioning, the diversity and distribution patterns of soil microbes at regional and global scales are far less understood than the respective distribution patterns of above-ground macro-organisms, such as plants and animals (Kazemi et al., 2016). The continuum of stages on glacier forefronts represents an ideal framework to study trajectories of microbial succession, as many glaciers have well-documented recession rates, and thus, the distance from the glacier provides a proxy of the time of the retreat, allowing for the examination of microbial succession along a spatial chronosequence (Walker et al., 2010).

Broad ecological differences between bacterial and fungal organisms, such as growth rates, stress tolerance and substrate utilization, suggest that they could follow distinct trajectories and show contrasting dynamics during ecosystem succession (Hannula et al., 2017). In fact, a number of studies have investigated the effects of environmental factors on soil microbial abundance and community structure at different scales. Intriguing results from the pioneering studies of Brown and Jumpponen (2014) and Cutler et al. (2014) showed that bacteria and fungi exhibit contrasting successional trajectories. Brown and Jumpponen (2014) claimed that bacterial succession was influenced more by plant establishment than by the succession of fungal communities during pedogenesis. Furthermore, the presence of plants but not the plant identity itself played a crucial role in structuring bacterial communities along the chronosequence. In contrast, Cutler et al. (2014) found that fungi were closely linked to plant establishment but bacteria were less so. Moreover, bacterial communities seemed to converge along the chronosequence, whereas no evidence of convergence was found in the fungal community. The reasons for this discrepancy are uncertain, and our understanding of the patterns and drivers of soil microbial communities remains limited, hampering generalizations on the basis of available studies.

Besides the bottom-up control of nutrient quality and quantity from altered vegetation, microbial communities are also influenced by top-down pressure from nematodes and other grazers (Wardle, 2006). Soil nematodes use an exceptionally wide range of resources and form functional groups at each trophic level, thereby holding a central position in the food web (Grandy et al., 2016). Therefore, the development of holistic models that include the full soil-plant-microbe-nematode complex will provide important clues for understanding the whole ecosystem development. Recent empirical and theoretical studies have highlighted that both stochastic and deterministic processes govern the spatial distribution of microbial communities at different spatial and temporal scales (Caruso et al., 2011). Neutrality-based theories emphasize that communities are stochastically assembled by probabilistic dispersal, ecological drift or historical inertia (Hubbell, 2001). In contrast, according to deterministic models, successional changes are directional, with dissimilarities among patches and successional rates decreasing over time, as communities converge towards similar stable states resistant to further colonization and invasion (Clark, 2009). The knowledge gap is particularly pronounced in understanding the relative importance of these two processes as drivers for bacterial and fungal assemblages. The clustering of bacteria along the Lyman Glacier Chronosequence suggested that bacterial communities are compiled in a more deterministic fashion than fungal communities (Brown and Jumpponen, 2014). In contrast, in a steppe ecosystem in North China, Zhang et al. (2011, 2016) argued that environmental changes affect the assembly of bacterial communities primarily through stochastic processes. However, most previous studies have focused on only a single group of organisms or a single trophic level (but see e.g., Soininen et al., 2007; Norfolk et al., 2015). Recently, Jonsson et al. (2016) investigated seven different groups or organisms and discovered a more deterministic pattern for beetle community changes, but a more stochastic pattern for litter fungal community changes along with the age of the ecosystem. It is reasonable to speculate that deterministic and stochastic processes can play different roles in contrasting organisms during different (early vs. late) successional stages (Powell et al., 2015; Jonsson et al., 2016).

93 However, current evidence is mostly based on descriptive approaches, which may limit the evaluation of the
94 relative importance between these two types of processes during ecosystem succession (Zhang et al., 2016).
95 The *Hailuogou Glacier Chronosequence* provides an excellent place to study the relationship between
96 vegetation succession and soil development, as its relatively mild and humid climate allows for rapid moraine
97 colonization by plants and promotes fast ecosystem development. Along the approximately 2 km-long belt, a
98 series of sites representing different stages of vegetation succession can be readily recognized, from a barren
99 stage supporting only some mosses to a lush forest stage. At this site, several studies have investigated specific
100 processes or organisms, such as pedogenesis (He and Tang, 2008; Zhou et al., 2013), plant succession (Zhong
101 et al., 1997; Yang et al., 2014), soil nematodes (Lei et al., 2015) and microbial changes (Sun et al., 2016a).
102 However, the understanding of the mechanistic underpinnings of community assembly is still highly
103 fragmentary, especially for the holistic soil-plant-microbe-nematode complex.
104 In this study, we used high-throughput Illumina paired-end sequencing of the bacterial small-subunit
105 ribosomal RNA (16S rRNA) gene and the fungal ribosomal internal transcribed spacer (ITS) to determine
106 both bacterial and fungal lineages associated with decadal scale stages of soil development in the *Hailuogou*
107 *Glacier Chronosequence*. Our main objectives were to disentangle fungal and bacterial successional dynamics
108 and community assembly as well as to decouple the effects of plant establishment, soil development and
109 nematode grazing on microbial successional trajectories. We hypothesized that: (1) bacterial and fungal
110 communities show hump-shaped responses to soil ageing, and the chronosequence enters into its retrogressive
111 phase after 120 years of succession mainly due to the decreased nutrient availabilities; (2) edaphic properties
112 serve as the primary agents in shaping bacterial communities, while the increasing abundance of lignin-rich
113 coniferous tree species at later stages of succession exerts a greater impact on fungal communities; (3)
114 stochastic processes dominate in microbial and microfauna community assemblages at the early stages, while
115 deterministic factors are more prevalent in plants and at the later stages. To the best of our knowledge, this is

among the first attempts to integrate knowledge of the soil-plant-microbe-nematode complex in a glacier forefield, and it may provide a breakthrough for a more holistic view of ecosystem development in the warmer and increasingly ice-free future world (Grandy et al., 2016).

2. Materials and methods

2.1. Study sites

The *Hailuogou Glacier Chronosequence* area has been described in detail in Zhou et al. (2013) and Lei et al. (2015). Briefly, the mean annual precipitation is about 2000 mm, with most (over 68%) occurring between June and October. The mean annual air temperature is 3.8 ºC, monthly averages ranging from -4.3 ºC in January (lowest) to 12.7 ºC in July (highest). The observed recession of the Hailuogou Glacier began in 1823, and it has accelerated markedly since the early 20th century. This study was conducted on seven sites undergoing long-term primary succession starting from bare soil, to pioneer communities and eventually to the climax vegetation communities at different ages after deglaciation and at different distances from the glacier terminus (Fig. S1; Lei et al., 2015). The approximate age for each stage studied was calibrated with chronologies according to tree-rings and soil erosion rates assessed by ^{137}Cs budget, and a seven-scale chronosequence (from stage 1, ca. 3 years since the glacier retreat, to stage 7, ca. 120 years; Fig. S1) was used.

2.2. Sampling design

At each chronosequence stage, three 5 × 5 m square experimental plots with a 10-m distance between the plots were established (except stages 1 and 2 where 2 × 2 m square plots with a 3-m distance between the plots were used due to the smaller area at the early stages). The taxa of plant communities were determined to the species level to assess plant richness, including tree, shrub and herb layers (Yang et al., 2014). If higher than 3 m, the tree biomass was calculated with the allometric equations reported by Zhong et al. (1997). The biomass of the shrub and herb layers was obtained through destructive sampling within the central 2 × 2 m of each subplot (Yang et al., 2014). All sampled plant material was sorted by species, and then oven-dried and weighted.

For soil sampling in mid-August 2016, a 50 × 50 cm quadrat was established in each of the three square

142 plots at each stage, and five soil cores were collected from the center and each corner of the quadrat using a
143 5-cm diameter soil corer after removal of litter from soil surface by hand. The five soil cores were combined
144 as one composite soil sample, and homogenized to pass through a 2-mm sieve after removing roots.
145 Approximately 200 g soil was divided into three parts and the material was used for (1) the analysis of soil
146 physicochemical properties, (2) the analysis of soil nematode communities, and (3) the estimation of soil
147 microbial biomass and extraction of DNA (stored at -80 ºC).
148
149 *2.3. Soil physicochemical properties and nematode community analyses*
150 The methods and data for soil physicochemical properties and nematode community analyses were as
151 detailed in Lei et al. (2015). Furthermore, the nematodes were identified to the genus level and the abundances
152 were assessed as a proxy for their biomass. Briefly, the nematodes were extracted from 100 g soil samples
153 using a modified cotton-wool filter method (McSorley and Frederick, 2004). The nematodes were killed at
154 70 °C in formaldehyde with 1% glycerol. The fixed nematodes were transferred to anhydrous glycerol
155 following the glycerol-ethanol method and mounted on a microscope slide. At least (when available) 150
156 nematodes from each sample were counted and identified to the genus level using an inverted compound
157 microscope.
158
159 *2.4. Microbial biomass assessments*
160 The microbial biomass was quantified by the chloroform-methanol extraction method based on Frostegård
161 et al. (1991). The phospholipids were transformed by alkaline methanolysis into fatty acid methyl esters, and
162 analyzed and quantified by a Hewlett-Packard 6890N-5973N gas chromatograph fitted with a 25 m capillary
163 column (Agilent 25 m × 0.2 mm inner diameter × 0.33 μm film thickness). The gas chromatography conditions
164 were set by the MIDI Sherlock program (MIDI, Inc. Newark, DE). The fatty acids i13:0, i15:0, a15:0, i16:0,

a17:0, i17:0, i19:0, 14:1ω5c, 15:1ω6c, 16:1ω7c, 16:1ω9c, 17:1ω8c, 18:1ω7c, 18:1ω9c, cy17:0 and cy19:0 were summed for calculating the bacterial biomass, while 16:1ω5c, 16:1ω11c and 18:2ω6 were summed to indicate the fungal biomass (Hortal et al., 2013).

2.5. Microbial DNA extraction and pyrosequencing

Soil genomic DNA was extracted from approximately 0.5 g soil per homogenized sample using the PowerSoil® DNA Isolation Kit (MoBio Laboratories, Inc., Carlsbad, USA) according to the manufacturer's instructions. The crude DNA extract was then purified by an UltraClean 15 DNA purification kit (MoBio, Carlsbad, CA, USA). DNA samples were diluted to 20 ng μl^{-1} before PCR amplification. The hypervariable regions V4-V5 of bacterial 16S rRNA genes were amplified using the barcode primers 515F (5′-GTGCCAGCMGCCGCGG-3′) and 907R (5′-CCGTCAATTCMTTTRAGTTT-3′), and the fungal ITS1 region was amplified by ITS1 (5'-CTTGGTCATTTAGAGGAAGTAA-3') and ITS2 (5'-GCTGCGTTCTTCATCGATGC-3') (Schoch et al., 2012; Sun et al., 2016b). The MiSeq Reagent Kit v3 was used to construct Illumina libraries according to the manufacturer's instructions. The PCR products from each sample were pooled and purified with QIAquick Gel Extraction kit (Qiagen), and high-throughput, paired-end sequencing was performed on the Illumina MiSeq PE300 platform.

2.6. Sequence analyses

The 1,282,898 and 1,400,981 raw sequences for bacteria and fungi, respectively, were processed using the pyrosequencing pipeline tools from the QIIME (http://qiime.sourceforge.net/) (Caporaso et al., 2010) and UPARSE software package (http://drive5.com/uparse/) (Edgar, 2013). Poor-quality sequences (shorter than 200 bp length, Phred quality score lower than 15 and any ambiguous nucleotides) were discarded from the dataset (Sun et al., 2016b). The remaining high-quality sequences were clustered to operational taxonomic

188 units (OTUs) through UPARSE-OTU, which is a novel 'greedy' algorithm that performs chimera filtering and
189 OTU clustering simultaneously, based on the 97% similarity level. The PyNAST tool was used to align all
190 selected representative sequences (De Santis et al., 2006). The bacterial sequences were classified using the
191 Greengenes database (http://greengenes.lbl.gov/), and sequences with no hits were designated "unclassified".
192 Fungal taxonomy was queried by UNITE fungal ITS reference databases (Bengtsson-Palme et al., 2013).
193 Bacterial and fungal sequences per sample were rarefied to 44,455 and 44,750 sequences, respectively, using
194 Good's coverage, Shannon index and Chao1 richness analyses. Relaxed neighbor-joining trees were generated
195 for each subsampled and aligned FASTA file using CLEARCUT (v.1.0.9), as embedded in MOTHUR
196 (Sheneman et al., 2006). Alpha diversity of soil bacterial and fungi was estimated by calculating the OTU
197 richness. To estimate the β-diversity in soil microbial communities, nonmetric multidimensional scaling
198 (NMDS) ordinations were generated using the R *vegan* package on the basis of Bray-Curtis dissimilarities.
199 Sequencing data for bacterial and fungal communities were deposited in the National Center for
200 Biotechnology Information (NCBI) Sequence Read Archive (http://trace.ncbi.nlm.nih.gov/Traces/sra/) under
201 the accession numbers of PRJNA354498 (bacteria) and PRJNA354828 (fungi).
202
203 *2.7. Parameter calculations and statistical analyses*
204 *Microbial network topological features* To better understand community structure, characterize intra-
205 community interactions and identify potential shared niches, the co-occurrence network analysis was
206 performed with the "igraph" R package. The 500 most abundant OTUs per chronosequence age were used to
207 build individual networks based upon a similar approach used by Dini-Andreote et al. (2014) and Sun et al.
208 (2017). Moreover, we also constructed networks using the most abundant 1000 OTUs to verify that the
209 interpretation of the trends of network properties did not change. For simplicity, networks were only given for
210 early (S1-2), middle (S3-5) and late (S6-7) stages. The numbers of nodes and edges, average degree and

clustering coefficient were calculated using the 'igraph' R package (Sun et al., 2017).

Indicator species analyses Microbial indicator species analyses were performed using the *multipatt* function implemented in the *indicspecies* package in R with 99 999 permutations and allowing combinations between habitats to identify OTUs leading to changes in multivariate patterns (Rime et al., 2015). For this analysis, single- and doubleton OTUs were removed as they hold little indicator information (Rime et al., 2015, 2016). Multiple testing corrections of *P*-values were performed using the *fdrtool* function, and indicator OTUs with $P < 0.05$ were considered significant.

Correlations of microbial community structures with environmental factors To further investigate the effect of edaphic (pH, soil density, soil moisture, soil organic carbon, total phosphorus, total nitrogen) and biotic properties (plant richness, aboveground and litter biomass, and litter C/N) on the bacterial and fungal communities, redundancy analysis (RDA) with the *vegan* R package (R Development, Core Team, 2013) was used. The factors' autocorrelation was excluded by using the *envfit* function in the *vegan* package before analyses. In addition, before the RDA analysis, a detrended correspondence analysis for the specific microbial groups was performed to confirm that the linear ordination method was appropriate for the analyses (gradient lengths < 3). The significance of the RDA model was tested by ANOVA based on 999 permutations (Oksanen et al. 2016; Sun et al., 2016b). Variance partitioning analysis (VPA) based on the redundancy analysis procedure was performed to quantify the relative contributions of environmental variables including biotic and edaphic factors using the *varpart* procedure in the R package *vegan* (Oksanen et al. 2016).

To visualize the complex relationships between microbial community richness and environmental variables, structural equation modeling (SEM) was used to identify the direct and indirect environmental effects. To simplify the model, we chose those characteristics strongly connected to bacterial and fungal richness, including edaphic factors (pH, total phosphorus and SOC), as well as biotic factors (plant richness and litter C/N). All included edaphic and biotic characteristics were subjected to logarithmic transformation

to meet the assumptions of normality. The SEM was conducted with the Amos 17.0 software package (Smallwaters Corporation, Chicago, IL, USA). The criteria for the evaluation of structural equation modeling fit, such as the *p*-values, χ^2 values, goodness-of-fit index (GFI) and the root mean square error of approximation (RMSEA), were adopted according to Hooper et al. (2008).

Successional trajectories of different organisms To detect the response direction and magnitude of plants, nematodes and microbial communities, we calculated the trends in changes in richness and biomass compared with stage 1, the base point. All variables were transformed using natural logarithmic transformation before the analyses.

Separating the respective importance of selection and chance effects The deterministic and stochastic changes were calculated as structural variations between every pair of plots using a modified method based on Zhang et al. (2011; 2016). Briefly, the structural variations for plant, nematode, bacterial and fungal communities were represented by Euclidean distances between the plots. The structural variation between plots at the initial stage S1 was taken as the base point, because that came merely from stochastic effects. Then, we calculated the effect of selection (S) = [(mean structural variation between S1 and the remaining six successional stages) - (base point)], and the effect of chance (C) = [(mean structural variation within the remaining six successional stage) - (base point)]. Both S and C might be positive or negative, corresponding to promoting or restraining structural changes, respectively, whereas their absolute values represent the magnitudes of their effects (Zhang et al., 2011). Then, for each successional stage, we calculated the importance of chance = $\frac{|C|}{|S|+|C|}$.

Changes in soil physicochemical characteristics, bacterial and fungal α-diversity, and the richness and biomass of plants, nematodes and microbial communities were also subjected to one-way analyses of variance (ANOVA) to determine the overall effects of chronosequence stages using SPSS 19.0 (SPSS Inc., Chicago,

256 IL). Significant differences among means were evaluated by Tukey's honest significant difference (HSD) at p

257 < 0.05.

3. Results

3.1. Changes in microbial community composition, structure and phylogenetic diversity

The relatively high Good's coverage values ranging from 0.985 to 0.991 suggested that microbial communities were well sampled owing to the high depth of Illumina sequencing (Table S1). After filtering and removing chimeras, clustering of the reads resulted in a total of 5584 bacterial (2432 ± 380 per sample) and 4838 fungal (814 ± 298 per sample) non-singleton OTUs. Based on the classifiable sequences, the bacterial reads were mostly assigned to eight phyla in the following order: Proteobacteria (44.19%), Acidobacteria (21.25%), Bacteroidetes (9.11%), Planctomycetes (4.1%), Actinobacteria (3.57%), Chloroflexi (3.10%), Gemmatimonadetes (2.34%) and Verrucomicrobia (2.03%) (Fig. 1a). The fungal community was dominated by the phyla Ascomycota (48.14%), Basidiomycota (36.84%) and Zygomycota (4.13%) (Fig. 1b).

The patterns of bacterial and fungal β-diversity were visualized with NMDS plots (Fig. 1c, d). The overall pattern of bacteria was differentiated into three clusters, stage 1 as cluster 1, stages 2–5 as cluster 2 and stages 6–7 as cluster 3, without overlapping among the three clusters across the chronosequence (Fig. 1c). In contrast, two clusters including early (stages 1–5) and late (stages 6–7) stages were separated for fungal communities (Fig. 1d). Compared with the fungi, tighter clustering was observed for the bacteria in each age class (Fig. 1c, d). Trends in relative proportions of some bacterial phyla were consistent across the chronosequence, including the continuous decreases in Bacteroidetes, and increases in Acidobacteria and Alphaproteobacteria. In contrast, fungal phyla were randomly distributed and no general pattern was found (Fig. S2).

3.2. Network topological characteristics and indicator species along the chronosequence

The topological properties of the co-occurrence networks showed that community complexity for both bacteria and fungi typically peaked at the middle chronosequence stages, as visible as the highest number of nodes and edges (Fig. 2; Table S2). Compared with bacteria, the higher clustering coefficients, and lower

281 nodes and edges in fungi implied that the fungal networks scattered across multiple small and discrete clusters
282 (Table S2). The overlapping nodes mainly belonged to bacterial groups Proteobacteria and Acidobacteria, and
283 fungal groups Ascomycota and Basidiomycota (Fig. 2). The most abundant 71 bacterial and 59 fungal OTUs
284 at the genus level were considered as indicator species (Fig. S3). OTUs associated with *Acidiferrobacter*,
285 *Geobacter*, *Hyphomicrobium*, *Polaromonas*, *Thiobacillus* (Proteobacteria) and *Arthobacter* (Actinobacteria)
286 were mainly found at the early stages 1 and 2. By contrast, Gp1, Gp2 and *Granulicella* (Acidobacteria),
287 *Bradyrhizobium*, *Burkholderia* and *Phenylobacterium* (Proteobacteria), and *Opitutus* (Verrucomicrobia)
288 mostly occurred at the last two stages. On the other hand, the middle three stages, including stages 3, 4 and 5,
289 harbored a variety of these bacteria (Figs. 2, S3). Among fungal indicators, *Massarina*, *Alternaria*, *Boeremia*,
290 *Mortierella*, *Mycoarthris*, *Neobulgaria* and *Otidea* were mainly present at the early stages, while *Sebacina*,
291 *Tomentella*, *Russula* and *Inocybe* appeared mostly at the later stages (Fig. S3b).
292
293 *3.3. Correlations of microbial communities with edaphic and biotic factors*
294 The availability of most nutrients increased along the chronosequence, including dissolved organic carbon
295 and total and inorganic (NH_4^+, NO_3^-) nitrogen, and similar patterns were also found for litter C/N and
296 aboveground biomass (Table S3). However, the total and bioavailable P concentration, as well as plant litter
297 biomass increased firstly until stage 3 and then decreased at the later stages (Table S3). Three clusters of
298 bacterial communities and two of fungal communities were differentiated by the redundancy analysis (Fig. 3a,
299 b). Furthermore, among the environmental factors, pH, total phosphorus, soil organic carbon as well as litter
300 C/N and plant richness were strongly related to microbial communities according to the length and angle of
301 axes (Fig. 3a, b). The variation partitioning analysis showed that edaphic properties were more important than
302 biotic factors in determining the bacterial and fungal community structure, especially at the early stages 1–5.
303 At the last two stages along with forest establishment, the importance of biotic factors as well as the interaction

304 of biotic and edaphic factors increased (Fig. 3c, d). Across the chronosequence, edaphic and biotic factors
305 explained 31.63 and 10.79% of bacterial variation, and 32.91 and 19.30% of fungal variation, respectively
306 (Fig. 3c, d).

307 The SEM models met the significance criteria according to their χ^2, p, AIC and RMSEA values (Fig. 3e,
308 f). Combining the direct and indirect effects, total absolute effects of environmental factors ranked according
309 to the following order: edaphic factors, total phosphorus (0.66), pH (0.64), SOC (0.44), and biotic factors,
310 plant richness (0.36) and nematode grazing (0.25) in bacteria, and SOC (0.62), fungal-feeding nematodes
311 (0.57), pH (0.52), plant richness (0.48) and total phosphorus (0.10) in fungi (Fig. 3e, f).

312

313 *3.4. Contrasting responses and driving forces in different groups of organisms*

314 Richness and biomass of the four organismal groups exhibited similar responses, yet distinct magnitudes
315 along the chronosequence (Fig. 4a, b). The most pronounced responses in richness were observed in plants
316 and nematodes, and the smallest responses in bacteria (Fig. 4a). On the other hand, biomass responses were
317 greatest in fungi, followed by bacteria, plants and nematodes (Fig. 4b). Most groups of organisms reached
318 their maximum richness at stage 5, maximum biomass at stage 6, and then the values decreased at the later
319 stages, except for the highest richness in bacteria observed at stage 2 and the continuous increase detected in
320 the biomass of plants (Fig. 4). An increase in the fungi/bacteria ratio as well as fungi-/bacteria-feeding
321 nematodes was observed in the last two stages (Fig. S4).

322 Stochastic processes dominated changes in bacterial and fungal communities, while deterministic
323 processes dominated the shaping of plant communities (Fig. 4c). In contrast, in nematodes, the deterministic
324 and stochastic processes were approximately equal (Fig. 4c). At the last two stages, the importance of
325 determinism increased for bacteria and fungi. Compared with bacteria, the fungal community composition
326 was more strongly driven by stochasticity (Fig. 4c).

4. Discussion

Microbial communities are the main drivers of organic matter decomposition to expedite pedogenesis, to facilitate the establishment of vascular plants, and to accelerate the successional dynamics of ecosystems (Bradley et al., 2016). According to a previous survey, the length of the growing season on the present study site is approximately 6 months, much longer than, for instance, the 3-month growing season of the Lyman Glacier area (Cázares et al., 2005). Therefore, the accumulation rates of organic C and N were 3–4 times and 7–11 times as high as those detected for other glacial chronosequences, respectively (He and Tang, 2008). The seven stages of the 120-year succession could be separated into three and two distinct clusters for bacterial and fungal communities, respectively (Figs. 1, 3). The pattern coincided with the vegetation dynamics: barren land with some mosses at stage 1, broadleaved shrubs and trees at stages 2–5, and lastly the climax stage with a coniferous *Abies fabri* and *Picea brachytyla* dominated forest at stages 6 and 7 (Lei et al., 2015). At the middle stages, the presence of more niches created by a greater plant diversity and, accordingly, a greater variety of organic substrates entering the soil, as well as less severe environmental stresses resulted in most diverse bacterial and fungal communities (Sun et al., 2016a; Table S1, 3; Figs. 1, 2). Most organismal groups of the plant-microbiota-nematode complex reached their maximum richness at stage 5 and maximum biomass at stage 6, after which the values decreased significantly (Fig. 4). Our findings were well in accordance with the Intermediate Disturbance Hypothesis, which states that the diversity of competing species is expected to be maximized at intermediate frequencies and intensities of disturbance or environmental changes (Connell, 1978).

4.1 Contrasting assemblage patterns for bacterial and fungal communities along the chronosequence

The co-occurrence networks analysis revealed that community complexity for both bacteria and fungi

typically peaked at the middle chronosequence stages, as indicated by the highest number of nodes and edges (Fig. 2; Table S2). Furthermore, compared with fungi, the lower clustering coefficients, and the higher nodes and edges in bacteria, implied a more compact topology with more direct paths of communication in the bacterial community (Figs. 1, 2; Table S2). The overlapping nodes mainly belonged to bacterial groups Proteobacteria and Acidobacteria, and fungal groups Ascomycota and Basidiomycota (Fig. 2), which may play critical ecological functions relating to ecosystem succession. This speculation was further supported by the indicator species analysis (Fig. S3). Indicator OTUs associated with *Acidiferrobacter*, *Geobacter*, *Hyphomicrobium*, *Polaromonas*, *Thiobacillus* (Proteobacteria), and *Arthobacter* (Actinobacteria) were mainly found at the early stages 1 and 2, as only these highly specialized organisms can thrive in an oligotrophic surrounding with extreme UV irradiation and temperature fluctuations (Rime et al., 2016). By contrast, Gp1, Gp2 and *Granulicella* (Acidobacteria), *Bradyrhizobium*, *Burkholderia* and *Phenylobacterium* (Proteobacteria), and *Opitutus* (Verrucomicrobia) mostly occurred at the last two stages. Meanwhile, some root-associated ectomycorrhizal fungi and other taxa capable of degrading complex organic C sources (Fig. S3; Rime et al., 2015), including *Phenylobacterium*, *Granulicella*, *Bradyrhizobium, Burkholderia* and *Opitutus* proliferated at later stages. At the middle stages, lower environmental stress and more niches created by the higher quantity and quality of plant species and litter contributed to the higher OTU richness and diversity (Sun et al., 2016a; Table S1, 2, 3; Figs. 2, 3).

The lower microbial OTU and plant species richness (Table S1; Fig. 4), as well as the significant decrease in nematode densities along with the disappearance of some rare genera of nematodes from higher trophic guilds (Lei et al., 2015) implied that stage 7 shows some declining characteristics, although this does not completely support our hypothesized retrogressive phase in the *Hailuogou Glacier Chronosequence* after 120 years of development. Moreover, the emerging retrogression might be largely related to the reduced bioavailability of phosphorus (Table S1), as soil microorganisms strongly compete with plants for the essential

373 nutrients (Zhou et al., 2013; Lei et al., 2015). Our findings were well in accordance with other findings
374 indicating that long-term reduction in the available P and transition from N to P limitation is the common
375 driver of retrogression across diverse systems (Peltzer et al., 2010). The strength of responses in phylogenetic
376 richness was greater for plants and nematodes than for fungi and bacteria, while most pronounced responses
377 in biomass were observed in fungi, followed by bacteria, plants, and lastly nematodes (Fig. 5). Thus, the
378 species richness of plants, as well as the biomass and phylogenetic structure of bacteria and fungi are sensitive
379 bioindicators, which could contribute to improved predictions of the direction and intensity of primary
380 succession in glacier forefields.
381
382 *4.2. Divergent driving forces for bacterial and fungal community assemblage along the chronosequence*
383 Variation partitioning analysis and structural equation models highlighted the different roles of edaphic
384 and biotic factors in determining soil bacterial and fungal richness (Fig. 3e, f). Generally, the edaphic
385 properties were more important than biotic factors in shaping the microbial communities, which is an expected
386 result given that the soil directly provides the substrate for the microbial communities. Our results are in
387 agreement with Chen et al. (2016), who observed that the variation in soil microbial communities in Tibetan
388 alpine grasslands was explained mainly by edaphic factors (soil organic carbon, C:N ratio, pH and soil texture),
389 and to a lower degree by biotic factors (aboveground biomass and plant richness), and even less by climatic
390 factors, including mean annual precipitation. These results provide strong support to the hypothesis that
391 edaphic factors are the dominant drivers of spatial variation in soil microbial communities at regional and
392 global scales.
393 In bacteria, the most prevailing ecological drivers seemed to be the soil pH, soil organic carbon and total
394 phosphorus, as assessed by their total effects (Fig. 3e). Indeed, there is growing evidence that soil pH
395 represents a key regulator in shaping the distribution of soil bacterial communities at regional scales (Fierer

396 and Jackson, 2006; Lauber et al., 2009). The apparent direct influence of soil pH on the bacterial community
397 composition is probably due to the narrow pH ranges for the optimal growth of bacteria (Cao et al., 2016).
398 Therefore, there was a shift in dominance from bacterial to fungal energy channels with an increasing soil age,
399 indicated by the increase in fungi/bacteria ratio as well as fungi-/bacteria-feeding nematodes at the last two
400 stages (Fig. S4), as a result of the higher tolerance to environmental changes for fungi (Bokhorst et al., 2017).
401 Meanwhile, soil organic matter sources have been routinely identified as having a pervasive effect on the
402 microbial communities, especially for bacteria (Vries et al., 2012). The explaining capacity of biotic factors
403 and the interaction of biotic and edaphic factors increased with the establishment of a coniferous forest at the
404 last two stages (Fig. 3c, d). Apart from serving as immediate decomposers, a large proportion of fungi can act
405 as endophytes, mutualists or pathogens with tight biotrophic interactions; therefore, it is assumed that there
406 would be a strong coupling of plant-fungal distribution patterns at regional scales (Wardle, 2006; Chen et al.,
407 2017). Our observations demonstrate that plants governed the turnover of soil fungal communities and
408 functional characteristics through the succession in the glacier retreat area, likely due to the continuous input
409 of detritus and differences in litter biochemistry among plant species (Fig. 3). Moreover, fungi-feeding
410 nematodes exerted more negative effects on fungal communities, thus creating a stronger top-down control
411 for fungi than bacteria (Fig. 3e, f), which also contributed to the dominance of biotic factors for fungal
412 assemblages.

413 Compared with bacteria, fungal communities are more determined by stochastic factors, as indicated by
414 the looser clustering (Figs. 2, 3) and higher importance of chance (Fig. 4). A likely explanation for this pattern
415 is that fungi might be dispersally more constrained than bacteria, and therefore more determined by historical
416 effects. In support of this hypothesis, Wilkinson et al. (2012) also showed that the 'propagule rain' of bacteria
417 smaller than 20 μm would reduce or eliminate the priority effects, thus resulting in a more deterministic
418 community assembly when compared to fungi. On the other hand, during the early stages, the patchy

distribution of soil resources accounts for the lottery of competition among microbial communities (Caruso et al., 2011). As the ecosystem develops over time, the increasing plant cover reduces heterogeneity in light and nutrient resources, and competition begins to play a dominant role, which would result in more deterministic processes. This was evidenced by the higher importance of selection at the later stages in both bacterial and fungal communities (Fig. 4c).

5. Conclusions

The bacterial and fungal communities exhibited dramatic differences in successional trajectories across the glacier chronosequence and also in the relative importance of driving deterministic vs. stochastic processes. Edaphic properties were the primary agents shaping the microbial community structures, especially at the early stages. The explaining capacity of biotic factors as well as the interactions between biotic and edaphic factors increased at the last two stages along with the increasing importance of forest cover, eventually governing the fungal turnover. Moreover, bacterial communities showed a more compact network topology during assembly, thus supporting determinism, whereas the looser clustering in fungal communities illustrated that they were more determined by stochastic processes. The biomass and phylogenetic structure of bacteria and fungi could be used as sensitive bioindicators for soil heath, enabling to make improved predictions of the rate, direction and magnitude of primary succession. In future studies, a model-data approach integrating field observations, laboratory incubations and elemental measurements as well as metagenomic analyses can expand our knowledge on the sensitivity and resilience of these fragile ecosystems under future environmental changes.

Acknowledgements The authors are grateful to the Gongga Mountain Alpine Ecosystem Observation Station,

Chinese Academy of Sciences for logistic support, and Genesky Biotechnologies Inc., Shanghai, China for help in sequencing and data analysis. This work was supported by the National Science Foundation of China (Nos. 31570598, 31370607 and 31100323) and the Talent Program of Hangzhou Normal University (2016QDL020).

References

Bokhorst, S., Kardol, P., Bellingham, P.J., Kooyman, R.M., Richardson, S.J., Schmidt, S., Wardle, D.A., 2017. Responses of communities of soil organisms and plants to soil aging at two contrasting long-term chronosequences. Soil Biology & Biochemistry 106: 69–79.

Bengtsson-Palme, J., Ryberg, M., Hartmann, M., Branco, S., Wang, Z., Godhe, A., De Wit, P., Sánchez-García, M., Ebersberger, I., de Sousa, F., Amend, A., Jumpponen, A., Unterseher, M., Kristiansson, E., Abarenkov, K., Bertrand, Y.J.K., Sanli, K., Eriksson, K.M., Vik, U., Veldre, V., Nilsson, R.H., 2013. Improved software detection and extraction of ITS1 and ITS2 from ribosomal ITS sequences of fungi and other eukaryotes for analysis of environmental sequencing data. Methods in Ecology & Evolution 4: 914–919.

Bradley, J.A., Arndt, S., Šabacká, M., Benning, L.G., Barker, G.L., Blacker, J.J., Yallop, M.L., Wright, K.E., Bellas, C.M., Telling, J., Tranter, M., Anesio, A.M., 2016. Microbial dynamics in a high-arctic glacier forefield: a combined field, laboratory, and modeling approach. Biogeosciences 13: 5677–5696.

Brown, S.P., Jumpponen, A., 2014. Contrasting primary successional trajectories of fungi and bacteria in retreating glacier soils. Molecular Ecology 23: 481–497.

Cao, P., Wang, J., Hu, H., Zheng, Y., Ge, Y., Shen, J., He, J., 2016. Environmental filtering process has more important roles than dispersal limitation in shaping large-scale prokaryotic beta diversity patterns of grassland soil. Microbial Ecology 72: 221–230.

Caporaso, J.G., Kuczynski, J., Stombaugh, J., Bittinger, K., Bushman, F.D., Costello, E.K., Fierer, N., Peña,

A.G., Goodrich, J.K., Gordon, J.I., Huttley, G.A., Kelley, S.T., Knights, D., Koenig, J.E., Ley, R.E., Lozupone, C.A., McDonald, D., Muegge, B.D., Pirrung, M., Reeder, J., Sevinsky, J.R., Turnbaugh, P.J., Walters, W.A., Widmann, J., Yatsunenko, T., Zaneveld, J., Knight, R., 2010. QIIME allows analysis of high-throughput community sequencing data. Nature Methods 7: 335–336.

Caruso, T., Chan, Y., Lacap, D.C., Lau, M.C., McKay, C.P., Pointing, S.B., 2011. Stochastic and deterministic processes interact in the assembly of desert microbial communities on a global scale. ISME Journal 5: 1406–1413.

Cázares, E., Trappe, J.M., Jumpponen, A., 2005. Mycorrhiza-plant colonization patterns on a subalpine glacier forefront as a model system of primary succession. Mycorrhiza 15: 405–416.

Chen, Y., Ding, J., Peng, Y., Li, F., Yang, G., Liu, L., Qin, S., Fang, K., Yang, Y., 2016. Patterns and drivers of soil microbial communities in Tibetan alpine and global terrestrial ecosystems. Journal of Biogeography 43: 2027–2039.

Chen, Y., Xu, T., Veresoglou, S.D., Hu, H., Hao, Z., Hu, Y., Liu, L., Deng, Y., Rillig, M.C., Chen, B., 2017. Plant diversity represents the prevalent determinant of soil fungal community structure across temperate grasslands in northern China. Soil Biology & Biochemistry 110: 12–21.

Clark, J.S., 2009. Beyond neutral science. Trends in Ecology and Evolution 24: 8–15.

Connell, J.H., 1978. Diversity in tropical rain forests and coral reefs - high diversity of trees and corals is maintained only in a non-equilibrium state. Science 199: 1302–1310.

Cutler, N.A., Chaput, D.L., van der Gast, C.J., 2014. Long-term changes in soil microbial communities during primary succession. Soil Biology & Biochemistry 69: 359–370.

De Santis, T.Z., Hugenholtz, P., Keller, K., Brodie, E.L., Larsen, N., Piceno, Y.M., Phan, R., Andersen, G.L., 2006. NAST: a multiple sequence alignment server for comparative analysis of 16S rRNA genes. Nucleic Acids Research 34: W394–W399.

488 Dini-Andreote, F., Silva, M.P.E., Triado-Margarit, X., Casamayor, E.O., van Elsas, J.D., Salles, J.F., 2014.
489 Dynamics of bacterial community succession in a salt marsh chronosequence: evidences for temporal niche
490 partitioning. ISME Journal 8:1989–2001.
491 Edgar, R.C., 2013. UPARSE: highly accurate OTU sequences from microbial amplicon reads. Nature Methods
492 10: 996–998.
493 Fierer, N., Jackson, R.B., 2006. The diversity and biogeography of soil bacterial communities. Proceeding of
494 the National Academy of Sciences of the United States of America 103: 626–631.
495 Frostegård, Å., Tunlid, A., Bååth, E., 1991. Microbial biomass measured as total lipid phosphate in soils of
496 different organic content. Journal of Microbiological Methods 14: 151–163.
497 Grandy, A.S., Wieder, W.R., Wichings, K., Kyker-Snowman, E., 2016. Beyond microbes: are fauna the next
498 frontier in soil biogeochemical model? Soil Biology & Biochemistry 102: 40–44.
499 Hannula, S.E., Morrien, E., de Hollander, M., van der Putten, W.H., van Veen, J.A., de Boer, W., 2017. Shifts
500 in rhizosphere fungal community during secondary succession following abandonment from agriculture.
501 ISME Journal 11: 2294–2304.
502 He, L., Tang, Y., 2008. Soil development along primary succession sequences on moraines of Hailuogou
503 glacier, Gongga Mountain, Sichuan, China. Catena 72: 259–269.
504 Hooper, D., Coughlan, J., Mullen, M., 2008. Structural equation modelling: guidelines for determining model
505 fit. Electronic Journal of Business Research Methods 6: 53–60.
506 Hortal, S., Bastida, F., Armas, C., Lozano, Y.M., Moreno, J.L., Garcia, C., Pugnaire, F.I., 2013. Soil microbial
507 community under a nurse-plant species changes in composition, biomass and activity as the nurse grows.
508 Soil Biology & Biochemistry 64: 139–146.
509 Hubbell, S.P., 2001. The unified neutral theory of biogeography and biodiversity. Princeton University Press,
510 Princeton, New Jersey, USA.

511 Jonsson, M., Snäll, T., Asplund, J., Clemmensen, K.E., Dahlberg, A., Kumordzi, B.B., Lindahl, B.D., Oksanen,
512 J., Wardle, D.A., 2016. Divergent responses of β-diversity among organism groups to a strong
513 environmental gradient. Ecosphere 7: e01535.
514 Kazemi, S., Hatam, I., Lanoil, B., 2016. Bacterial community succession in a high-altitude subarctic glacier
515 foreland is a three-stage process. Molecular Ecology 25: 5557–5567.
516 Lauber, C.L., Hamady, M., Knight, R., Fierer, N., 2009. Pyrosequencing-based assessment of soil pH as a
517 predictor of soil bacterial community structure at the continental scale. Applied and Environmental
518 Microbiology 75: 5111–5120.
519 Lei, Y., Zhou, J., Xiao, H., Duan, B., Wu, Y., Korpelainen, H., Li, C., 2015. Soil nematode assemblages as
520 bioindicators of primary succession along a 120-year-old chronosequence on the Hailuogou Glacier
521 forefield, SW China. Soil Biology & Biochemistry 88: 362–371.
522 McSorley, R., Frederick, J.J., 2004. Effect of extraction method on perceived composition of the soil nematode
523 community. Applied Soil Ecology 27, 55–63.
524 Norfolk, O., Eichhorn, M.P., Gilbert, F.S., 2015. Contrasting patterns of turnover between plants, pollinators
525 and their interactions. Diversity and Distributions 21: 405–415.
526 Oksanen, J., Blanchet, F.G., Friendly, M., Kindt, R., Legendre, P., McGlinn, D. Minchin, P.R., O´Hara, R.B.,
527 Simpson, G.L., Solymos, P.S., Stevens, M.H., Szoecs, E., Wagner, H., 2016. Package 'vegan'. http://www.r-
528 project.org, http://vegan.r-forge.r-project.org/.
529 Peltzer, D.A., Wardle, D.A., Allison, V.J., Baisden, W.T., Bardgett, R.D., Chadwick, O.A., Condron, L.M.,
530 Paritt, R.L., Porder, S., Richardson, S.J., Turner, B.L., Vitousek, P.M., Walker, J., Walker, L.R., 2010.
531 Understanding ecosystem retrogression. Ecological Monographs 80: 509–529.
532 Powell, J.R., Karunaratne, S., Campbell, C.D., Yao, H.Y., Robinson, L., Singh, B.K., 2015. Deterministic
533 processes vary during community assembly for ecologically dissimilar taxa. Nature Communications 6:

8444.

R Core Team., 2013. R: A Language and Environment for Statistical Computing. R Foundation for Statistical Computing. http://www.r-project.org.

Rime, T., Hartmann, M., Brunner, I., Widmer, F., Zeyer, J., Frey, B., 2015. Vertical distribution of the soil microbiota along a successional gradient in a glacier forefield. Molecular Ecology 24: 1091–1108.

Rime, T., Hartmann, M., Frey, B., 2016. Potential sources of microbial colonizers in an initial soil ecosystem after retreat of an alpine glacier. ISME Journal 10: 1625–1641.

Schoch, C.L., Seifert, K.A., Huhndorf, S., Robert, V., Spouge, J.L., Levesque, C.A., Chen, W., Fungal Barcoding Consortium, 2012. Nuclear ribosomal internal transcribed spacer (ITS) region as a universal DNA barcode marker for Fungi. Proceedings of National Academy of Sciences of the United States of America 109: 6241–6246.

Sheneman, L., Evans, J., Foster, J.A., 2006. Clearcut: a fast implementation of relaxed neighbor joining. Bioinformatics 22: 2823–2824.

Soininen, J., Lennon, J.J., Hillebrand, H., 2007. A multivariate analysis of beta diversity across organisms and environments. Ecology 88: 2830–2838.

Sun, H., Wu, Y., Zhou, J., Bing, H., 2016a. Variations of bacterial and fungal communities along a primary successional chronosequence in the Hailuogou glacier retreat area (Gongga Mountain, SW China). Journal of Mountain Science 13: 1621–1631.

Sun, R., Dsouza, M., Gilbert, J.A., Guo, X., Wang, D., Guo, Z., Ni, Y., Chu, H., 2016b. Fungal community composition in soils subjected to long-term chemical fertilization is most influenced by the type of organic matter. Environmental Microbiology 18: 5137–5150.

Sun, S., Li, S., Avera, B.N., Strahm, B.D., Badgley, B.D., 2017. Soil bacterial and fungal communities show distinct recovery patterns during forest ecosystem restoration. Applied and Environmental Microbiology 83:

557 e00966-17.
558 Vries, F.T., Manning, P., Tallowin, J.R.B., Mortimer, S.R., Pilgrim, E.S., Harrison, K.A., Hobbs, P.J., Quirk,
559 H., Shipley, B., Cornelissen, J.H.C., Kattge, J., Bardgett, R.D., 2012. Abiotic drivers and plant traits explain
560 landscape-scale patterns in soil microbial communities. Ecology Letters 15: 1230–1239.
561 Walker, L.R., Wardle, D.A., Bardgett, R.D., Clarkson, B.D., 2010. The use of chronosequences in studies of
562 ecological succession and soil development. Journal of Ecology 98: 725–736.
563 Wardle, D.A., 2006. The influence of biotic interactions on soil biodiversity. Ecology Letters 9, 870–886.
564 Wilkinson, D.M., Koumoutsaris, S., Mitchell, E.A.D., Bey, I., 2012. Modeling the effect of size on the aerial
565 dispersal of microorganisms. Journal of Biogeography 39: 89–97.
566 Yang, Y., Wang, G.X., Shen, H.H., Yang, Y., Cui, H.J., Liu, Q., 2014. Dynamics of carbon and nitrogen
567 accumulation and C:N stoichiometry in a deciduous broadleaf forest of deglaciated terrain in the eastern
568 Tibetan Plateau. Forest Ecology & Management 312: 10–18.
569 Zhang, X., Johnston, E.R., Liu, W., Li, L., Han, X., 2016. Environmental changes affect the assembly of soil
570 bacterial community primarily by mediating stochastic processes. Global Change Biology 22: 198–207.
571 Zhang, X., Liu, W., Bai, Y., Zhang, G., Han, X., 2011. Nitrogen deposition mediates the effects and importance
572 of chance in changing biodiversity. Molecular Ecology 20: 429–438.
573 Zhong, X., Luo, J., Wu, N., 1997. Researches of the forest ecosystems on Gongga Mountain. Chengdu
574 University of Science and Technology Press, Chengdu.
575 Zhou, J., Wu, Y., Prietzel, J., Bing, H., Yu, D., Sun, S., Luo, J., Sun, H., 2013. Changes of soil phosphorus
576 speciation along a 120-year soil chronosequence in the Hailuogou Glacier retreat area (Gongga Mountain,
577 SW China). Geoderma 195–196: 251–259.

578 **Figure captions**

579 **Figure 1.** Taxonomic proportions and nonmetric multidimensional scaling (NMDS) ordinations of bacterial

(a, c) and fungal (b, d) diversities at different successional stages along the *Hailuogou Glacier Chronosequence*.

Figure 2. Co-occurrence network analysis of bacterial and fungal communities at different successional stages along the *Hailuogou Glacier Chronosequence*.

Figure 3. Redundancy ordinations (a, b), variation partitioning analysis (c, d) and structural equation modeling (e, f) of the selected environmental variables for microbial community structures along the *Hailuogou Glacier Chronosequence*. AP, available phosphorus; SOC, soil organic carbon; TN, total nitrogen; TP, total phosphorus. In e and f, solid and dashed arrows represent positive and negative correlations, respectively. The thickness of the arrows reflects the magnitude of the standardized coefficients. GFI, goodness-of-fit index; RMSEA, root mean square error of approximation.

Figure 4. Responses of richness (a), biomass (b) and the relative importance of change effect (C) in different groups of organisms at different successional stages along the *Hailuogou Glacier Chronosequence*. Different letters indicate significant differences ($p < 0.05$) among seven successional stages according to Tukey's HSD for one-way ANOVA.

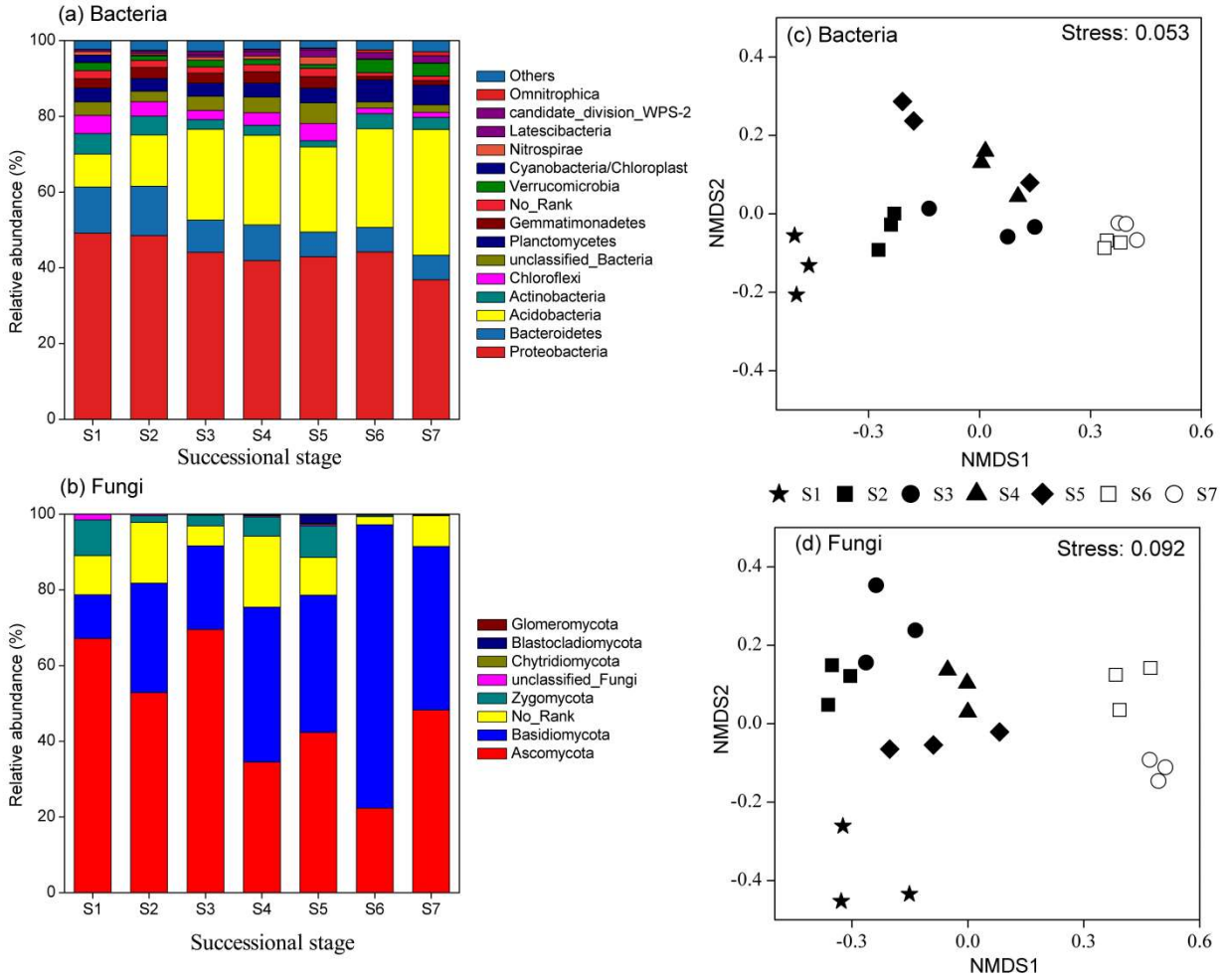

595

596 **Figure 1.**

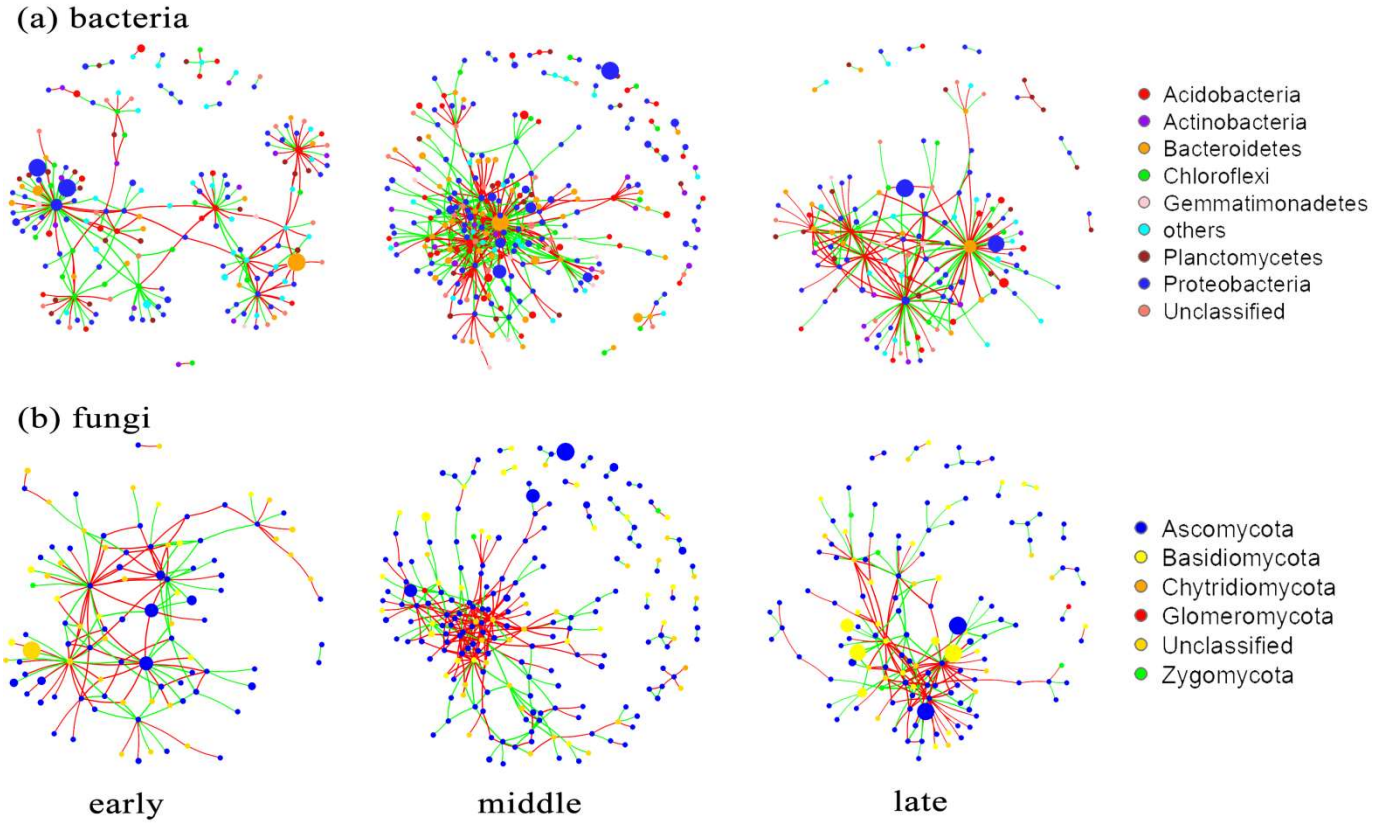
(a) bacteria
Acidobacteria
Actinobacteria
Bacteroidetes
Chloroflexi
Gemmatimonadetes
others
Planctomycetes
Proteobacteria
Unclassified
(b) fungi
Ascomycota
Basidiomycota
Chytridiomycota
Glomeromycota
Unclassified
Zygomycota
early
middle
late

Figure 2.

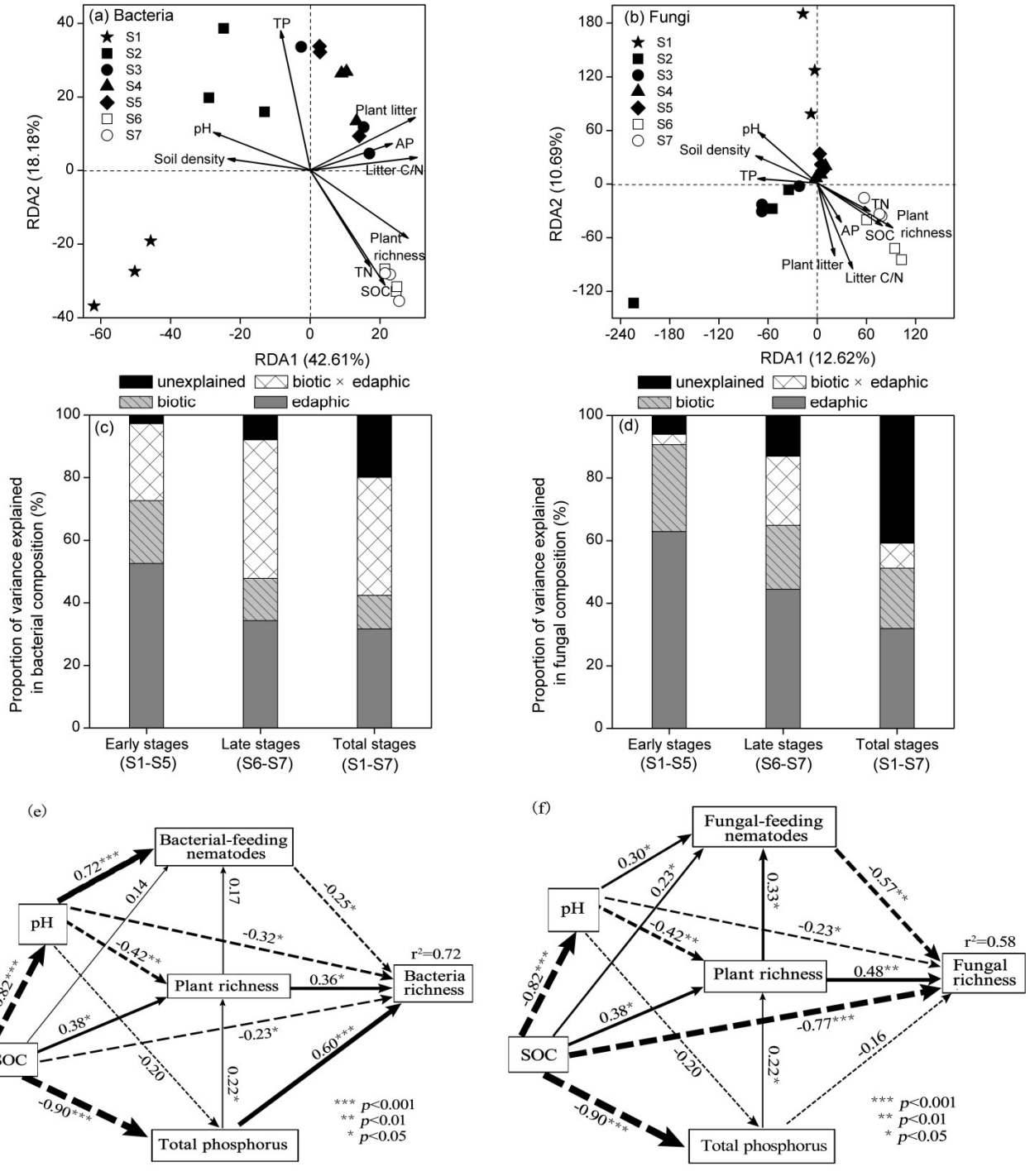
(a) Bacteria
S1
S2
S3
S4
S5
S6
S7
TP
Plant litter
pH
AP
Soil density
Litter C/N
Plant richness
TN
SOC
RDA2 (18.18%)
RDA1 (42.61%)
(b) Fungi
RDA2 (10.69%)
RDA1 (12.62%)
unexplained
biotic × edaphic
biotic
edaphic
(c)
Proportion of variance explained in bacterial composition (%)
Early stages (S1-S5)
Late stages (S6-S7)
Total stages (S1-S7)
(d)
Proportion of variance explained in fungal composition (%)
(e)
Bacterial-feeding nematodes
Plant richness
Bacteria richness
r²=0.72
Total phosphorus
*** p<0.001
** p<0.01
* p<0.05
χ²=2.002, df=2, P=0.368, AIC=40.002, GFI=0.969, RMSEA=0.006
(f)
Fungal-feeding nematodes
Fungal richness
r²=0.58
χ²=3.286, df=2, P=0.219, AIC=43.221, GFI=0.945, RMSEA=0.025

Figure 3.

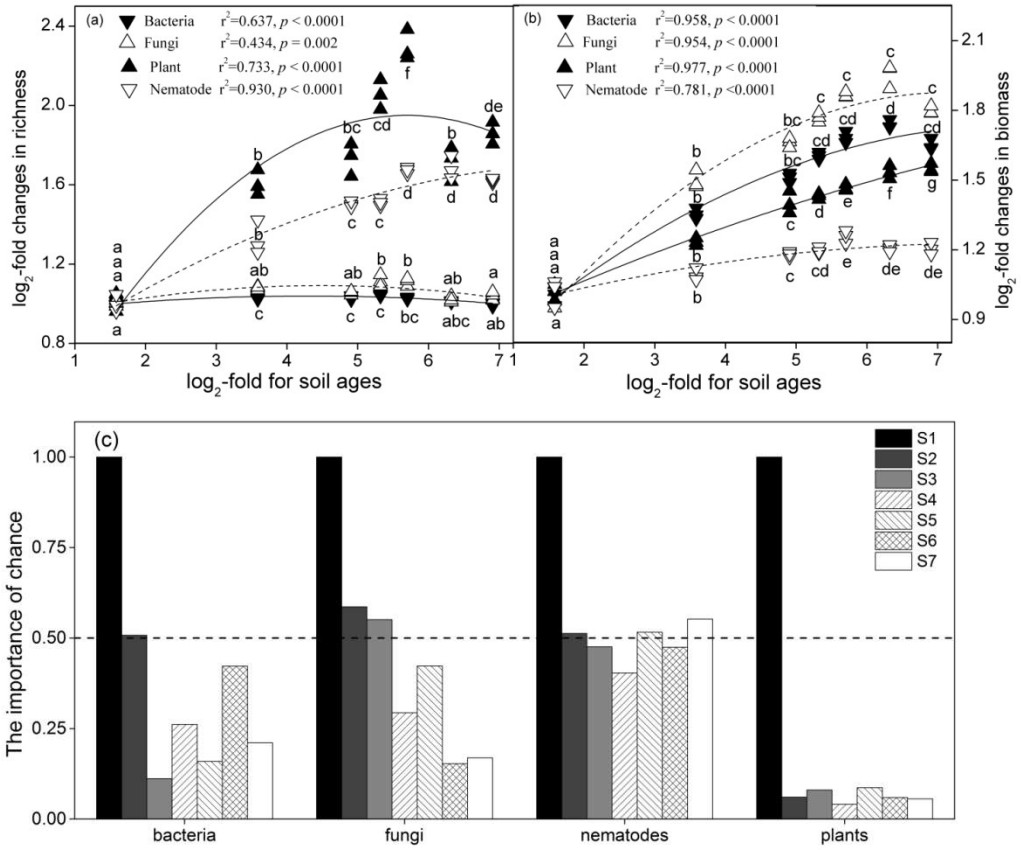

602

603 **Figure 4.**